Proceedings of the 2001 IEEE
International Conference on Robotics & Automation
Seoul, Korea • May 21-26, 2001

Manipulability Analysis for Mobile Manipulators

B. Bayle*, J.-Y. Fourquet** and M. Renaud*
* *LAAS-CNRS, Toulouse, France*
** *ENIT, Tarbes, France*
{bbayle, renaud}@laas.fr and fourquet@enit.fr

Abstract

We extend the standard definition of manipulability to the case of a nonholonomic mobile manipulator built from an n joint robotic arm and a nonholonomic mobile platform. The effects of mounting the arm on a nonholonomic platform are shown through the analysis of the manipulability thus defined. Applications of criteria inherited from manipulability considerations are given to justify design and to generate the controls of our system.

1 Introduction

Mobile manipulator is nowadays a widespread term to refer to robots built from a robotic arm mounted on a mobile platform. Such systems allow the more usual missions of robotics systems which require both *locomotion and manipulation* abilities [1]. Actually, such systems combine the advantages of mobile platforms and robotic arms and reduce their drawbacks. For instance, the mobile platform extends the arm workspace, whereas an arm offers many operational functionalities (simply opening a door for the robot...). Although appeared very early in the robotics history [2] [3], this concept has mainly been studied for less than ten years [4] [5] [6] [7] [8]. Most publications address problems inherited from robotic arms state of art, such as control [4] [6], path optimization [5] or operational path following [7] [8]. In spite of the great variety of the problems to be solved and the corresponding publications [9], quite few efforts have been made on the modelling. Among the few references, we can cite Tchoń and Muszyński [10]. When the mobile manipulator has an *holonomic* platform, the arm modelling can be directly applied. In the case of a wheeled mobile platform, the rolling without slipping of the wheels on the floor involves a different modelling. The mobile platform cannot move instantly in any arbitrary direction, due to this constraint. It is then said to be *nonholonomic* and it is necessary to consider specific properties of mobile platforms [11].

Our study has been motivated by the generation of the mobile manipulator velocities to execute a given operational path [12], for example to paint a complex surface. The inversion of the direct instantaneous kinematic model of the mobile manipulator allows us to solve this problem and to take into account some additional criteria, since our system is redundant (see section 4). As a usual criterion, we consider the *manipulability measure* due to Yoshikawa [13] [14], which is very useful to characterize the instantaneous kinematics of a given system. *This study aims at understanding the use of this concept, usually defined for robotic arms, in the case of mobile manipulators.*

In section 2 we will introduce a generic modelling of mobile manipulators built from a two independent driven wheels platform. Then, in section 3, we will recall the theory of manipulability based on the singular value decomposition and we will apply it to mobile manipulators. Section 4 will point out some possible applications of this instantaneous kinematic analysis.

2 Modelling of a Mobile Manipulator

In the general case we consider a mobile manipulator built from an n joint robotic arm mounted on a nonholonomic mobile platform (see figure 1). Let $\mathcal{R} = (O,\ \vec{x},\ \vec{y},\ \vec{z})$ be the fixed frame of world coordinates and $\mathcal{R}' = (O',\ \vec{x'},\ \vec{y'},\ \vec{z'})$ be the moving frame attached to the platform. Furthermore, let $\mathcal{R}_0 = (O_0,\ \vec{x}_0,\ \vec{y}_0,\ \vec{z}_0)$ be the moving frame attached to the arm base. The position of the arm base, with respect to the platform, is defined by two parameters a and b (see figure 1). Let $\mathcal{R}_n = (O_n,\ \vec{x}_n,\ \vec{y}_n,\ \vec{z}_n)$ be a moving frame attached to the arm end effector. The point O_{n+1}, which is the center of the end effector, is fixed relative to the frame $\mathcal{R}_n$.

If we leave the wheels out of account we can identify the three *generalized coordinates of the platform* $\mathbf{q}_p$ (defining its *configuration*) with the three *operational coordinates* $\boldsymbol{\xi}_p$ (defining its *location*). A classical choice is $\boldsymbol{\xi}_p = [\xi_{p1}\ \xi_{p2}\ \xi_{p3}]^T = [x\ y\ \vartheta]^T$ (see figure 1). The controls on this platform are repre-

0-7803-6475-9/01/$10.00 © 2001 IEEE

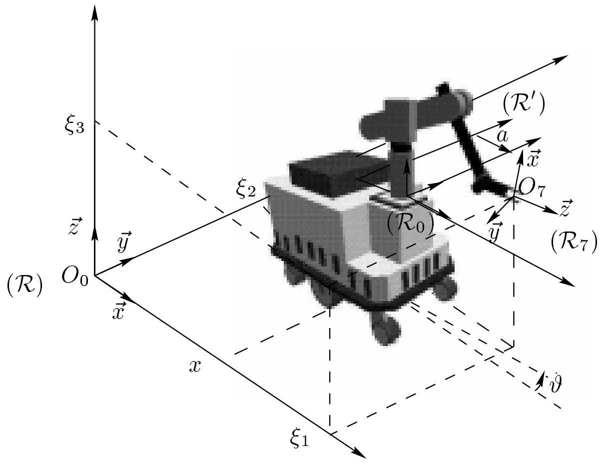

Figure 1: Mobile manipulator H2BIS ($n = 6$ and $b = 0$)

sented by $\mathbf{u}_p = [u_{p1}\ u_{p2}]^T = [v\ \omega]^T$ in which v and ω represent respectively the linear and angular velocities of the platform. The *configuration instantaneous kinematic model* [15] of this platform is $\dot{\mathbf{q}}_p = S(\mathbf{q}_p)\mathbf{u}_p$, with:

$$S(\mathbf{q}_p) = \begin{bmatrix} \cos\vartheta & 0 \\ \sin\vartheta & 0 \\ 0 & 1 \end{bmatrix}.$$

As we explained in the introduction, the instantaneous kinematics of the platform is constrained by the rolling without slipping of the wheels on the floor. This nonholonomic (or non integrable) constraint can be written in the form:

$$G_p(\mathbf{q}_p)\dot{\mathbf{q}}_p = 0, \tag{1}$$

with $G_p(\mathbf{q}_p) = [\sin\vartheta \quad -\cos\vartheta \quad 0]$.

The *configuration of the arm* is defined by the n *generalized coordinates*: $\mathbf{q}_a = [q_{a1}\ q_{a2}\ \dots\ q_{an}]^T$, and the end effector *location* (i.e. the position of the point O_{n+1} and the orientation of the frame $\mathcal{R}_n$, relative to $\mathcal{R}_0$), by the m *operational coordinates*: $\boldsymbol{\xi}_a = [\xi_{a1}\ \xi_{a2}\ \dots\ \xi_{am}]^T$. The *direct kinematic model* of the arm, relative to $\mathcal{R}_0$, is $\boldsymbol{\xi}_a = f_a(\mathbf{q}_a)$ and the *direct instantaneous kinematic model* is:

$$\dot{\boldsymbol{\xi}}_a = J_a(\mathbf{q}_a)\dot{\mathbf{q}}_a, \tag{2}$$

with $J_a(\mathbf{q}_a) = \frac{\partial f_a(\mathbf{q}_a)}{\partial \mathbf{q}_a}$.

Thus, the *configuration of the mobile manipulator* is defined by $\nu = n + 3$ *generalized coordinates*: $\mathbf{q} = [q_1\ q_2\ \dots\ q_\nu]^T = [x\ y\ \vartheta\ q_{a1}\ q_{a2}\ \dots\ q_{an}]^T$. From equation (1) it is then possible to write:

$$G(\mathbf{q})\dot{\mathbf{q}} = 0, \tag{3}$$

with $G(\mathbf{q}) = \begin{bmatrix} G_p(\mathbf{q}_p) & 0 \end{bmatrix}$. Also, we can characterize the end effector *location*, (i.e. the position of the point O_{n+1} and the orientation of the frame $\mathcal{R}_n$, relative to $\mathcal{R}$), by the μ *operational coordinates* $\boldsymbol{\xi} = [\xi_1\ \xi_2\ \dots\ \xi_\mu]^T$. The direct kinematic model of the mobile manipulator relative to $\mathcal{R}$, is $\boldsymbol{\xi} = f(\mathbf{q})$ and the direct instantaneous kinematic model is:

$$\dot{\boldsymbol{\xi}} = J(\mathbf{q})\dot{\mathbf{q}}, \tag{4}$$

with $J(\mathbf{q}) = \frac{\partial f}{\partial \mathbf{q}}$. From equations (3) and (4), all the velocities constraints are:

$$\begin{bmatrix} G(\mathbf{q}) \\ J(\mathbf{q}) \end{bmatrix} \dot{\mathbf{q}} = \begin{bmatrix} 0 \\ \dot{\boldsymbol{\xi}} \end{bmatrix}.$$

Let $\mathbf{u} = [\mathbf{u}_p^T\ \dot{\mathbf{q}}_a^T]^T$ be the vector of the velocities for the system. Then $\dot{\mathbf{q}} = M(\mathbf{q})\mathbf{u}$, with:

$$M(\mathbf{q}) = \begin{bmatrix} S(\mathbf{q}_p) & 0 \\ 0 & I_n \end{bmatrix},$$

where I_n is the n order identity matrix. Taking into account that $G(\mathbf{q})M(\mathbf{q}) = 0$, we obtain:

$$\dot{\boldsymbol{\xi}} = \bar{J}(\mathbf{q})\mathbf{u}, \tag{5}$$

with $\bar{J}(\mathbf{q}) = J(\mathbf{q})M(\mathbf{q})$.

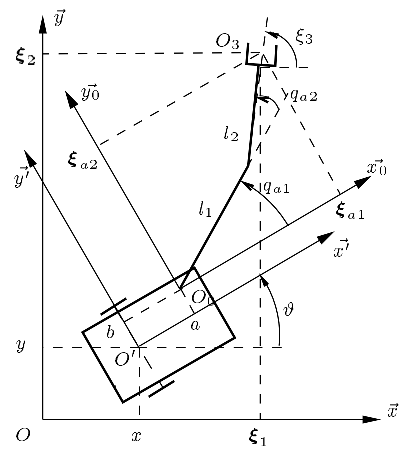

Figure 2: A planar mobile manipulator ($n = 2$)

Example: a planar mobile manipulator Let us consider an horizontal double pendulum mounted on the platform (see figure 2 and [8]); its configuration is defined by $\mathbf{q} = [x\ y\ \vartheta\ q_{a1}\ q_{a2}]^T$ and so $\nu = 5$. In the frame $\mathcal{R}$, the position of the point O_3 is given by the Cartesian coordinates ξ_1 and ξ_2 and the orientation of the end effector by the angle ξ_3; then $\mu = 3$ (see figure 2). Here, $\mathbf{u} = [v\ \omega\ \dot{q}_{a1}\ \dot{q}_{a2}]^T$ and the matrix $\bar{J}(\mathbf{q})$ becomes:

$$\bar{J}(\mathbf{q}) = \begin{bmatrix} C_3 & D_3 & D_2 & D_1 \\ S_3 & D_6 & D_5 & D_4 \\ 0 & 1 & 1 & 1 \end{bmatrix},$$

with the following variables, using a quasi-minimum number of operations:

$$\begin{array}{ll} S_3 = \sin q_3 & D_1 = -l_2 S_{345} \\ C_3 = \cos q_3 & D_2 = -l_1 S_{34} + D_1 \\ S_{34} = \sin(q_3 + q_4) & D_3 = -aS_3 - bC_3 + D_2 \\ C_{34} = \cos(q_3 + q_4) & D_4 = l_2 C_{345} \\ S_{345} = \sin(q_3 + q_4 + q_5) & D_5 = l_1 C_{34} + D_4 \\ C_{345} = \cos(q_3 + q_4 + q_5) & D_6 = aC_3 - bS_3 + D_5 \end{array}$$

3 Manipulability analysis

3.1 Some results on the manipulability of a robotic arm

This section introduces elements of the manipulability theory as developed by Yoshikawa. For more precisions or full demonstrations, the reader may refer to [16].

Let us consider a robotic arm and its direct instantaneous kinematic model $\dot{\boldsymbol{\xi}}_a = J_a(\mathbf{q}_a)\dot{\mathbf{q}}_a$.

Theorem 3.1 *The subset of the realizable operational velocities $\dot{\boldsymbol{\xi}}_a$ such that the corresponding joint velocity verifies $||\dot{\boldsymbol{q}}_a|| \leq 1$ is an ellipsoid in the m-dimensional space containing $\dot{\boldsymbol{\xi}}_a$.*

Elements of proof The general solution to invert the instantaneous kinematics of the arm can be written as:

$$\dot{\mathbf{q}}_a = J_a^+(\mathbf{q}_a)\dot{\boldsymbol{\xi}}_a + (I_n - J_a^+(\mathbf{q}_a)J_a(\mathbf{q}_a))\mathbf{z},$$

where $\mathbf{z}$ is any vector of dimension n and $J_a^+(\mathbf{q}_a)$ the pseudoinverse of $J_a(\mathbf{q}_a)$. This stands if and only if $\dot{\boldsymbol{\xi}}_a \in Im(J_a(\mathbf{q}_a))$, i.e. for regular configurations. We can show that the condition $||\dot{\mathbf{q}}_a|| = \dot{\mathbf{q}}_a^T \dot{\mathbf{q}}_a \leq 1$ leads to the equivalent condition $\dot{\boldsymbol{\xi}}_a^T (J_a^+(\mathbf{q}_a))^T J_a^+(\mathbf{q}_a)\dot{\boldsymbol{\xi}}_a \leq 1$, which represents an ellipsoid in the operational velocities space. □

Theorem 3.2 *Let $J_a(\boldsymbol{q}_a) = U_a(\boldsymbol{q}_a)\Sigma_a(\boldsymbol{q}_a)V_a^T(\boldsymbol{q}_a)$ be the Singular Value Decomposition (SVD) of matrix $J_a(\boldsymbol{q}_a)$ [17]. $U_a(\boldsymbol{q}_a)$ and $V_a(\boldsymbol{q}_a)$ are orthogonal and $\Sigma_a(\boldsymbol{q}_a)$ has the ordered singular values on its diagonal. Let us assume that $U_a(\boldsymbol{q}_a) = [\boldsymbol{u}_1\ \boldsymbol{u}_2\ \dots\ \boldsymbol{u}_m]$ and that the singular values are $\sigma_{a1} \geq \sigma_{a2} \geq \dots \geq \sigma_{am}$. Then, the main axes of the manipulability ellipsoid are given by $\sigma_{a1}\boldsymbol{u}_1$, $\sigma_{a2}\boldsymbol{u}_2, \dots, \sigma_{am}\boldsymbol{u}_m$ and its volume is proportional to the product $\sigma_{a1}\sigma_{a2}\dots\sigma_{am}$.*

Elements of proof *To simplify writings, we hide the dependence on $\boldsymbol{q}_a$ for this proof.*

Let us apply the SVD of J_a to $\dot{\boldsymbol{\xi}}_a^T (J_a^+)^T J_a^+ \dot{\boldsymbol{\xi}}_a \leq 1$. We easily get that it is equivalent to:

$$(U_a^T \dot{\boldsymbol{\xi}}_a)^T (\Sigma_a^+)^T V_a^T V_a \Sigma_a^+ (U_a^T \dot{\boldsymbol{\xi}}_a) \leq 1.$$

As V_a is orthogonal, we can simplify the previous inequality: $\tilde{\dot{\boldsymbol{\xi}}}_a^T (\Sigma_a^+)^T \Sigma_a^+ \tilde{\dot{\boldsymbol{\xi}}}_a \leq 1$, where $\tilde{\dot{\boldsymbol{\xi}}}_a = U_a^T \dot{\boldsymbol{\xi}}_a$. Moreover, as:

$$\Sigma_a^+ = \begin{bmatrix} 1/\sigma_{a1} & 0 & 0 & \dots & \dots & 0 \\ 0 & 1/\sigma_{a2} & 0 & \dots & \dots & 0 \\ \dots & \dots & \dots & \dots & \dots & \dots \\ 0 & \dots & \dots & \dots & 0 & 1/\sigma_{am} \\ 0 & 0 & 0 & 0 & 0 & 0 \\ \dots & \dots & \dots & \dots & \dots & \dots \\ 0 & 0 & 0 & 0 & 0 & 0 \end{bmatrix},$$

the initial inequality finally writes [1]:

$$\sum_{\sigma_{ai} \neq 0} \frac{(\tilde{\dot{\boldsymbol{\xi}}}_a)_i}{\sigma_{ai}}^2 \leq 1,$$

which is the equation of an ellipsoid. Its main axes are given by the $u_i, i = 1, 2, \dots, m$ with the associated radii σ_{ai}. □

Thanks to this theoretical bases we can analyze the instantaneous kinematics of a robotic arm from different points of view. The visualization of the ellipsoid may be interesting but of course it only applies when the operational space is 2-D or 3-D. So, one often considers only positioning of the end effector. The shape of the manipulability ellipsoid (ellipse in a planar case), gives an information on the capabilities of the arm to move in the different directions of the operational space.

Additionally, we can define different algebraic measures to characterize this ellipsoid. They are often called *manipulability measures* and give a monodimensional information. The more usual manipulability measure is $w = \sigma_{a1}\sigma_{a2}\dots\sigma_{am}$, which is proportional to the ellipsoid volume. It thus gives a quantitative information on the manipulability. Moreover it can be shown that $w = \sqrt{\det(J_a(\mathbf{q}_a)J_a^T(\mathbf{q}_a))}$ which simplifies into $w = |\det J_a(\mathbf{q}_a)|$ when $J_a(\mathbf{q}_a)$ is square: it is not necessary to apply the SVD to compute w.

If we look for a more qualitative information, we can compute the ratio of the minimum and maximum radii of the ellipsoid: $w_2 = \frac{\sigma_{am}}{\sigma_{a1}}$. Yoshikawa underlines that it is the reciprocal of the *condition number* (numerical information to evaluate the distance to singularities) of the Jacobian $J_a(\mathbf{q}_a)$, which is an interesting computational feature. In this article, we choose to define a manipulability measure[2] extending the notion of *eccentricity* of the ellipse: $w_5 = \sqrt{1 - \frac{\sigma_{am}^2}{\sigma_{a1}^2}}$.

[1] Notice that $1/\sigma_{ai}$ is replaced by 0 if $\sigma_{ai} = 0$.

[2] We call this measure w_5 as Yoshikawa defines four other measures: w, w_2, w_3 and w_4.

Example If we consider only the double pendulum robotic arm of our planar mobile manipulator (see section 2) for a positioning task, we can illustrate the different previous items. We could represent the manipulability ellipses of this arm all around its workspace. Rather, we examine the evolution of manipulability when the end effector position follows a straight line from an extended position ($q_{a1} = q_{a2} = 0$) to the origin ($q_{a1} = \frac{\pi}{2}, q_{a2} = -\pi$). Figure 3 displays the manipulability measure w_5 based on the ellipses eccentricity, as a function of the arm extent, similarly as Yoshikawa [16]. It gives informations on the shape of the ellipses. Indeed, as w_5 decreases to 0 the possible end effector velocities are becoming more isotropic. Also, $w_5 = 0$ would mean that the end effector can move equally in any direction with a bounded velocity control vector.

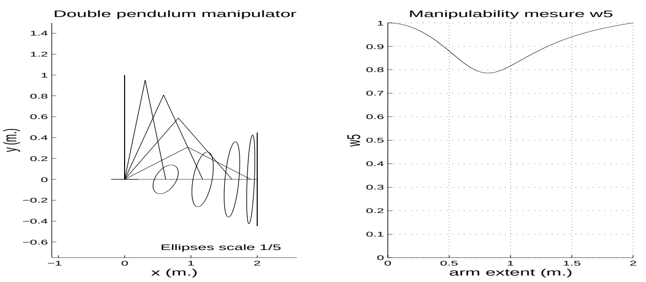

Figure 3: Manipulability analysis for the robotic arm

We note that, in the case of the robotic arm, there are two singularities in our simulations, when $\mathbf{q}_a = [0\ 0]^T$ and $\mathbf{q}_a = [\frac{\pi}{2}\ \ -\pi]^T$. Indeed we show that $\det J_a(\mathbf{q}_a) = 0$ in both configurations, which implies $w = 0$, and thus $\sigma_{am} = 0$, which implies $w_5 = 1$. On figure 3, it corresponds to a degenerated ellipse.

3.2 Case of mobile manipulators

We now take into account the mobile platform. With the proposed modelling (see section 2), we can apply a similar strategy to define manipulability. Let us consider the demonstrations done in subsection 3.1 with the direct instantaneous model of a robotic arm (see equation (2)). They use the Jacobian of the robotic arm: $J_a(\mathbf{q}_a)$. Let us apply the same demonstrations to the mobile manipulator using the model linking $\dot{\boldsymbol{\xi}}$ to $\mathbf{u}$ (see equation (5)). It is easy to understand that those proofs hold with matrix $\bar{J}(\mathbf{q})$. However, $\bar{J}(\mathbf{q})$ is not a Jacobian matrix as $\mathbf{u}$ is not the derivative of $\mathbf{q}$. According to the same idea, we can extend the notion of singularity for the mobile manipulator. A configuration of the mobile manipulator will be said to be *singular* if $\text{rank}(\bar{J}(\mathbf{q})) \neq \max_{\mathbf{q}} \text{rank}(\bar{J}(\mathbf{q}))$. Also the manipulability ellipsoids do not correspond to the inequality $||\dot{\mathbf{q}}|| \leq 1$ but to $||\mathbf{u}|| \leq 1$, which is slightly different[3]. It is logical not to use the derivative of the configuration, as the platform is nonholonomic. Yet, we could have considered the wheels velocities rather than the linear and angular velocities, but this is strictly equivalent. In most cases, controllers for nonholonomic mobile platforms use linear and angular velocities, and then, an appropriate transformation gives the wheels configurations. However the quantitative result would have been a little different using the wheels velocities in place of v and ω.

It is not generally possible (except perhaps for some special cases) to separate analytically the effects of the platform and the arm. So, to get aware of the effects of the mobile platform we propose different numeric simulations.

Example We still consider the example of the planar mobile manipulator, with $a = b = 0$, i.e. with the arm base in the middle of the wheels axis. We use the same simulation conditions as in the previous example (see section 3.1), but now the arm is mounted on the mobile platform (see figure 4). The effects of the mobile platform on the shape of the produced ellipses and the manipulability measure are relevant.

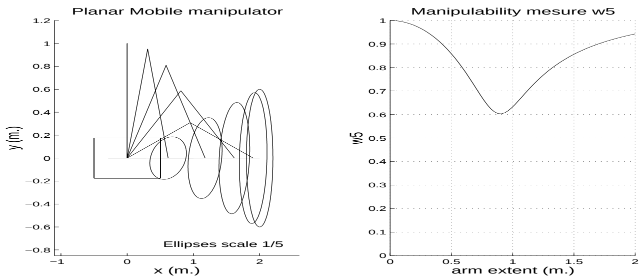

Figure 4: Manipulability analysis for the mobile manipulator

The platform contributes to the manipulability of the system: in the case of the mobile manipulator, the manipulability ellipse is no longer flat when $q_{a1} = 0$ and $q_{a2} = 0$ if $\vartheta = 0$ (compare figures 3 and 4). This means that the mobile manipulator manipulability does not vanish in this configuration.

As noticed by Yamamoto and Yun [18], the manipulability then reflects the constraints on the system. So, as the platform is not holonomic its effects on the movement is not equal in any direction of the workspace. This can be pointed out if we leave the

[3] There are two differences: the definition and the value: $\mathbf{u}$ is not the derivative of the configuration vector as usual in the manipulability theory and $||\dot{\mathbf{q}}|| \neq ||\mathbf{u}||$.

arm fully extended and we play on the first joint of the arm (see figure 5).

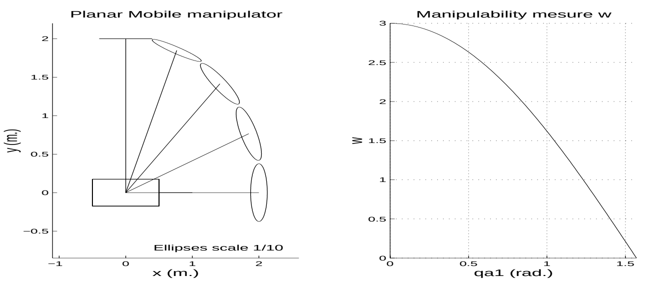

Figure 5: Manipulability analysis: effects of the nonholonomic constraint

When the arm is stretched in the wheels axis direction, the arm, considered alone, is in a singular configuration. The mobile platform cannot instantly move in a direction perpendicular to its main axis because of the nonholonomic constraint. Indeed, by solving $\det \bar{J}(\mathbf{q})\bar{J}^T(\mathbf{q}) = 0$, we get the singular configurations: if $a = b = 0$, $q_{a1} = \frac{\pi}{2} \mod (\pi), \forall\ q_{a2}$. Thus, if the first link of the robotic arm is parallel to the y axis the system is singular (see figure 5). In the other cases it is not anymore.

4 Applications

4.1 Applications to mobile manipulator design

Manipulability can be used to design a robotic system, through parameter optimization, in some precise purpose. Gardner and Velinsky [19] introduce numeric comparisons that allow them to choose the position of the arm base on the platform, given a robot structure (a 3 DOF anthropomorphic robotic arm mounted on a wheeled mobile platform) and a particular task (straight line path on an highway). Another aspect that could help controllers design is dealt with by Yamamoto and Yun [18]. They normalize the Jacobian matrix to evaluate the effects of maximum linear velocity of the platform on manipulability of the system. This can be useful to size the platform motoring.

A quantitative analysis permits to obtain the effects of the arm base position on the platform. Indeed, we can compare manipulability ellipses shape for different value of the parameters a and b. Notably, we can consider the effect of $a \neq 0$. Let us consider the case of the planar mobile manipulator again. If $a \neq 0$, the platform allows the mobile manipulator to move in the direction of the wheel axis, whatever the configuration of the arm (see figure 6).

Another remark can be done concerning the orientation of the arm on the platform. As we are aware that the contribution of the mobile platform is maximum in the direction of the longitudinal axis of the platform, it is a better choice to choose this direction as the middle of the first joint configurations range. This applies when the first joint of the robotic arm is a vertical rotod joint, which is quite common.

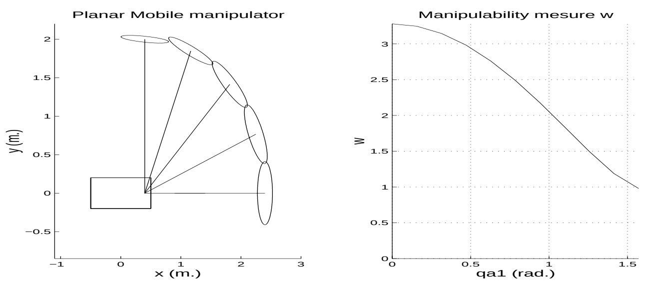

Figure 6: Manipulability analysis: effects of the nonholonomic constraint

4.2 Applications to mobile manipulator control

In [12] we proposed an inversion scheme to solve the redundancy of the mobile manipulator ($\nu > \mu$) and obtain a particular generalized path for the mobile manipulator when its end effector path is given. From a instantaneous kinematics point of view we can translate this coordination strategy into:

$$\mathbf{u} = \bar{J}^{+}(\mathbf{q})\dot{\boldsymbol{\xi}} - W(I_{\nu-1} - \bar{J}^{+}(\mathbf{q})\bar{J}(\mathbf{q}))\left(\frac{\partial \mathcal{P}(\mathbf{q})}{\partial \mathbf{q}} M\right)^T,$$

where W is positive weighting matrix and $\mathcal{P}(\mathbf{q})$ a scalar function depending on the configuration of the system. This function was initially built from the classical manipulability measure w (see section 3.1). It was based on the analytical expression of the *arm* manipulability measure. Two elements must now be taken into account:

- through our previous results (section 3.2), it would now be more consistent to use the *mobile manipulator* manipulability measure. Yet, depending on the application we may have to consider the whole system manipulability or the robotic arm manipulability (for instance when the mobile manipulator is not used in a coordinated fashion strategy). If the user wants to keep the platform motionless to manipulate with the arm alone, it would be convenient to reach the operating site in a good configuration for the arm, from a manipulation point of view. So, generally, we can consider:

$$\mathcal{P}(\mathbf{q}) = \alpha(\mathbf{q})\mathcal{P}_{p+a}(\mathbf{q}) + (1 - \alpha(\mathbf{q}))\mathcal{P}_a(\mathbf{q}_a),$$

the convex combination of two functions based on the arm manipulability: $\mathcal{P}_a(\mathbf{q}_a)$ and the mobile manipulator manipulability: $\mathcal{P}_{p+a}(\mathbf{q})$. The smooth scalar function $\alpha(\mathbf{q}) \in [0\ 1]$ allows to adapt the choice of the criteria to the configuration of the mobile manipulator;

- the analytical expression of the manipulability of a mobile manipulator system, even simple, can be complex. It may not be helpful to design the $\mathcal{P}(\mathbf{q})$ function. Rather it would be more interesting to consider functions of manipulability with minimum corresponding to optimal configurations, such as w^{-1} or w_5, and to compute their numeric gradient.

5 Conclusion

In this article, we analyzed the instantaneous kinematic modelling of a particular class of wheeled mobile manipulators subject to nonholonomic constraints. We showed how the notion of manipulability can be extended in that case to represent the possible operational motions in a given configuration of the system. Some simulations give an idea of the effects of the platform on the shape of manipulability ellipses, with an obvious dependence on nonholonomy. We discussed how manipulability can be used as a criterion to design or to control a mobile manipulator. An interesting aspect to develop this study could be to deal with the dynamics of the problem, that can be treated as a dual problem (duality velocity–forces) [16], or through dynamic modelling [18].

References

[1] T. Arai. Robots with integrated locomotion and manipulation and their future. In *IROS'96*, pages 541–545, Osaka, Japan, November 1996.

[2] V. Pavlov and A. Timofeyev. Construction and stabilization of programmed movements of a mobile robot-manipulator. *Engineering Cybernetics*, 14(6):70–79, 1976.

[3] P. Spampinato, L. Masson, K. Watts, N. Grant, and D. Kuban. Three equipment concepts for the fusion engineering device. *Transactions of the American Nuclear Society*, 43:765, 1982.

[4] K. Liu and F. Lewis. Decentralized continuous robust controller for mobile robots. In *ICRA'90*, pages 1822–1826, Cincinnati, USA, May 1990.

[5] F. G. Pin and J.-C. Culioli. Multi-criteria position and configuration optimization for redundant platform/manipulator systems. In *IEEE Workshop on Intelligent Robots and Systems*, pages 103–107, July 1990.

[6] N. A. M. Hootsmans and S. Dubowsky. Large motion control of mobile manipulators including vehicle suspension characteristics. In *ICRA'91*, pages 2336–2341, Sacramento, USA, April 1991.

[7] Y. Yamamoto and X. Yun. Coordinating locomotion and manipulation of a mobile manipulator. In *Conference on Decision and Control*, pages 2643–2648, Tucson, USA, December 1992.

[8] H. Seraji. An on-line approach to coordinated mobility and manipulation. In *ICRA'93*, pages 28–35, Atlanta, USA, May 1993.

[9] B. Bayle, J.-Y. Fourquet, and M. Renaud. Manipulateurs mobiles : Problématiques et état de l'art (in french). Technical Report n. 00087, LAAS–CNRS, Toulouse, France, March 2000.

[10] K. Tchoń and R. Muszyński. Instantaneous kinematics and dexterity of mobile manipulators. In *ICRA'2000*, pages 2493–2498, San Francisco, USA, April 2000.

[11] G. Foulon, J-Y. Fourquet, and M. Renaud. Coordinating mobility and manipulation using nonholonomic mobile manipulators. *Control Engineering Practice*, 7:391–399, 1999.

[12] B. Bayle, J.-Y. Fourquet, and M. Renaud. A coordination strategy for mobile manipulation. In *IAS'2000*, pages 981–19988, Venice, Italy, July 2000.

[13] T. Yoshikawa. Analysis and control of robot manipulators with redundancy. In M. Brady and R. Paul, editors, *Robotics Research: The First International Symposium*, pages 735–747. MIT Press, 1984.

[14] T. Yoshikawa. Manipulability of robotic mechanisms. *International Journal of Robotics Research*, 4(2):3–9, 1985.

[15] G. Campion, G. Bastin, and B. D'Andra-Novel. Structural properties and classification of kinematic and dynamic models of wheeled mobile robots. *IEEE Transactions on Robotics and Automation*, 12(1):47–62, February 1996.

[16] T. Yoshikawa. *Foundations of Robotics : Analysis and Control*. The MIT Press, 1990.

[17] G. Golub and C. Van Loan. *Matrix Computations*. Johns Hopkins University Press, 1996.

[18] Y. Yamamoto and X. Yun. Unified analysis on mobility and manipulability of mobile manipulators. In *ICRA'99*, pages 1200–1206, Detroit, USA, May 1999.

[19] J. Gardner and S. Velinsky. Kinematics of mobile manipulators and implications for design. *Journal of Robotic Systems*, 17(6):309–320, 2000.